Aerosol Science and Technology, 41:1089–1101, 2007
Copyright © American Association for Aerosol Research
ISSN: 0278-6826 print / 1521-7388 online
DOI: 10.1080/02786820701697812

Photothermal Interferometric Aerosol Absorption Spectrometry

Arthur Sedlacek and Jeonghoon Lee
Brookhaven National Laboratory, Atmospheric Sciences, Upton, New York, USA

Aerosol light absorption still remains a difficult quantity to measure at the precision, accuracy and temporal resolution necessary to quantitatively bound the contribution of this direct effect on aerosol radiative forcing. These continuing difficulties are due, in part, because aerosol extinction is dominated by light scattering. In response to these and other issues, the aerosol community has been developing a new generation of instrumentation that can measure aerosol absorption without the need to deposit aerosols on a filter. Here we introduce work on the application of photothermal interferometry (PTI) towards this measurement problem. The advantages of this approach are: its complete insensitivity to aerosol scattering (true for any photothermal technique) and high sensitivity resulting from use of an interferometric technique. Using NO_2 as a calibration standard, the accuracy of the PTI technique was measured to be 5% (95% confidence interval). Measurement at a 10-second time constant yields a precision of 0.2 Mm^{-1} (95% confidence interval) and a lower limit of detection of 0.4 Mm^{-1} for a sample pathlength of 5 cm. Using laboratory-generated nigrosin aerosols an intercomparison between the PTI and a 3-λ Particle Soot Absorption Photometer (PSAP) gives a slope of 0.96 ± 0.02. Acquisition of absorption coefficients for ambient aerosols reveals very good agreement between the two instruments except for periods of high relative humidity (>70%) whereupon the PSAP reports a larger absorption coefficient.

INTRODUCTION

A more quantitative understanding of the direct, indirect, and semi-direct effects needs to be developed to more completely understand the impact of aerosol forcing on climate change (Charlson 1991, 1992; Kaufman et al. 2002; Vinoj et al. 2004; Hansen et al. 1997, 1998; Lohman and Feichter 2001). This need was recently emphasized by Schwartz (2004) who stated that aerosol forcing needs to "be reduced by at least three-fold for uncertainty in climate sensitivity to be meaningfully reduced and bounded." Despite much work on the aerosol direct effect, much uncertainty still remains regarding the importance of aerosol absorption. This is due, in large part, to the uncertainties associated with commonly available instruments for measuring aerosol absorption. Furthermore, since aerosol forcing can be of a magnitude comparable to those induced by anthropogenically released greenhouse gases, quantifying the ratio of aerosol absorption to scattering is critical to quantifying conditions under which aerosols offset GHG emissions [cooling effect] and when they contribute to warming.

Extinction of solar radiation occurs through both absorption and scattering which is readily quantified using the Beer-Lambert Law,

$$T = \exp(-\sigma_{\text{ext}}^{\text{total}} l), \qquad [1]$$

where T is the transmission, $\sigma_{\text{ext}}^{\text{total}}$ is the total extinction coefficient and l is the path length. Here the total extinction includes solar flux losses through scattering and absorption by gases ($\sigma_{\text{scat}}^{\text{gas}}$ and $\sigma_{\text{abs}}^{\text{gas}}$) and aerosols ($\sigma_{\text{scat}}^{\text{aer}}$ and $\sigma_{\text{abs}}^{\text{aer}}$). Since radiative transfer properties are sensitive to aerosol absorption through the ratio of aerosol scattering to total extinction (Charlson 1992; Chylek and Wong 1995; Haywood et al. 1995, 1999) a unitless parameter, referred to as the single scattering albedo (SSA), is often used:

$$\bar{\omega} = \frac{\sigma_{\text{scat}}^{\text{aer}}}{\sigma_{\text{ext}}^{\text{aer}}} = \frac{\sigma_{\text{scat}}^{\text{aer}}}{\sigma_{\text{abs}}^{\text{aer}} + \sigma_{\text{scat}}^{\text{aer}}}. \qquad [2]$$

Ambient values for $\bar{\omega}$ can range from 1 for pure particle scattering to a rarely observed 0.5 for a strongly absorbing aerosol. However, values for SSA typically range from 1 to 0.8. In light of the strong sensitivity of forcing on $\bar{\omega}$, it is often convenient to report on aerosol absorption through the single scattering

Received 27 April 2007; accepted 22 September 2007.
The authors would like to gratefully acknowledge Dr. Mike Downs (Interferomet, Ltd.) for the many insightful discussions and e-mails and John Hubbe (Pacific Northwest National Laboratory) for making the 3-wavelength PSAP available for this study. This study was supported by the Atmospheric Science Program within the Climate Change Research Division, U.S. Department of Energy under contract no. DE-AC02-98CH10886 and NASA/Atmospheric Composition program under contract No. NNH06AD30I. Partial support for JL was provided by the KICOS-Battelle Internship Program.
Address correspondence to Arthur Sedlacek, Environmental Sciences Department, Atmospheric Sciences Division, Brookhaven National Laboratory, Upton, NY 11973-5000, USA. E-mail: sedlacek@bnl.gov

co-albedo (η),

$$\eta = 1 - \bar{\omega} = \frac{\sigma_{\text{abs}}^{\text{aer}}}{\sigma_{\text{ext}}^{\text{aer}}} = \frac{\sigma_{\text{abs}}^{\text{aer}}}{\sigma_{\text{abs}}^{\text{aer}} + \sigma_{\text{scat}}^{\text{aer}}} \approx \frac{\sigma_{\text{abs}}^{\text{aer}}}{\sigma_{\text{scat}}^{\text{aer}}} \quad \left(\text{for } \sigma_{\text{abs}}^{\text{aer}} \ll \sigma_{\text{scat}}^{\text{aer}}\right). \qquad [3]$$

The co-albedo is simply the fraction of local extinction due to absorption, which, in the limit of very weak absorption, reduces to the ratio of aerosol absorption to scattering.

Superficially, the measurement of $\sigma_{\text{abs}}^{\text{aer}}$ would appear to be straightforward: measure the total extinction (i.e., sample transmission) and remove contributions due to Rayleigh scattering, molecular absorption (species dependent) and, finally, aerosol scattering. At present, the most commonly used methods try to do just this, either by monitoring light transmission as a function of material deposited onto a filter and correcting for multiple scattering effects due to the filter substrate or by taking the difference between aerosol extinction and scattering. However, in practice, procurement of $\sigma_{\text{abs}}^{\text{aer}}$ with uncertainty levels that enable the bounding of the direct effect on radiative forcing is not so straightforward.

The most widely used method for measuring the absorption coefficient is to deposit the particulates onto a filter and monitor the decrease in the transmission of light (Lin et al. 1973; Campbell et al. 1995; Bond et al. 1999; Anderson et al. 2003; Virkkula et al. 2005). The numerous advantages of this approach include commercial availability (e.g., the Particle Soot Absorption Photometer (PSAP) by Radiance Research); unattended operation; a robust, low-tech method; and a relatively fast response time (ca. 30 seconds). However, filter-based approaches have drawbacks that warrant caution when used. Chief among these cautions is artifact absorption, which originates because particulate and/or filter substrate light scattering can cause light to scatter outside the detection field of view (FOV) as well as provide the scattered photons a second (or third) chance to be absorbed by the deposited aerosol. Both processes will, absent careful calibration, result in an over-estimate of the true absorption. This specific issue was addressed by Bond and co-workers (Bond et al. 1999) where it was reported that all filter-based measurements of aerosol absorption display some response to scattering by particles. Specifically, it was found that filter-based techniques possess a response to scattering that ranges from 2–9%, depending upon the particular technique employed [PSAP, Integrating Plates (IP) or Hybrid Integrating Plate System (HIPS)]. In the case of the PSAP, this sensitivity to scattering (2%) was exhibited after the application of an empirical calibration that accounts for enhanced absorption due to the filter medium, and for nonlinearities in the response of the unit as the filter is loaded, the so-called calibration transfer coefficient. Such residual sensitivity to aerosol scattering could become a significant problem for the filter-based measurement scheme when $\bar{\omega}$ is very near unity. Despite the scattering correction, aerosol absorption measured via these filter methods on reference samples was still found to be too large by 20–30%. These artifacts can be largely corrected for using the Bond coefficients: K_1 and K_2 (Bond et al. 1999). In addition, other harder to quantify effects can also potentially compromise the absorption coefficient reported by PSAP-like instruments. For example, evaporation of semi-volatile material off the particle following collection could result in a non-negligible change in the absorption coefficient due to the loss of a transparent coating on top of a black carbon (BC) core. Alternatively, hygroscopic particles could wet the filter material causing the transmittance through the filter to increase through a "wet T-shirt effect" (Schwartz 2003). However, even this wetting process is not straightforward since the hydrophilic nature of the cellulose substrate that supports the glass fiber used to trap the particles could cause the cellulose substrate to swell and act as a shutter (Arnott et al. 2003). Finally, since the PSAP measures the change in intensity (I) with respect to time, it can be shown that the measurement noise for this differential technique will go as $t^{-3/2}$ (Springston and Sedlacek 2007). The consequence of this is that the noise level for the reported absorption coefficients will increase at a faster rate than a direct measurement where the noise follows $1/\sqrt{t}$ and this can become an issue when fast instrument response is required. While these effects will only manifest themselves when absorption is very small, it is often precisely these ambient conditions that are of greatest interest, though there are other sampling scenarios where the noise can severely degrade the data even under large absorption coefficient conditions (Springston and Sedlacek 2007). It is also noted that the multi-angle absorption photometry (MAAP) approach developed by Petzold and co-workers (2002, 2004) has demonstrated success at overcoming some of the artifactual absorption issues and is available commercially (Thermo Scientific, Waltham, MA).

Another commonly used method for measuring aerosol light absorption is the difference method, where the difference between the aerosol extinction and scattering is taken. The work of Strawa et al. (2003), and others (Moosmüller et al. 2005; Smith and Atkinson 2001; Vander Wal and Ticich 1999; Sappey et al. 1998 employing the cavity ringdown (CRD) technique represents a state-of-the-art example of this approach. These groups use the CRD technique to measure the particle extinction and, in some cases, have incorporated a nephelometer-type scattering measurement channel into the instrument (Hallar and Strawa 2004). However, the seemingly straightforward data reduction warrants care. Here the chief concern centers on the extraction of a small number, $\sigma_{\text{abs}}^{\text{aer}}$, from two, large and nearly identical numbers (e.g., $\sigma_{\text{ext}}^{\text{aer}} - \sigma_{\text{scat}}^{\text{aer}}$). As a specific example, suppose $\bar{\omega} = 0.9$ and there is 5% uncorrelated error in the measurement of $\sigma_{\text{ext}}^{\text{aer}}$ and $\sigma_{\text{scat}}^{\text{aer}}$, as might be expected from a combination of the cavity ringdown technique and a nephelometer. The uncertainty in $\sigma_{\text{abs}}^{\text{aer}}$, for this approach, would be (Bevington 1969)

$$\delta_{\text{abs}}^2 = \delta_{\text{ext}}^2 + \delta_{\text{scat}}^2, \qquad [4]$$

where δ represents the absolute uncertainty and the subscripts are as defined above. It can be shown (Strawa et al. 2003) that

the relative uncertainty in σ_{abs}^{aer} is

$$\left(\frac{\delta_{abs}}{\sigma_{abs}^{aer}}\right)^2 = \left(\frac{1}{\eta}\frac{\delta_{ext}}{\sigma_{ext}^{aer}}\right)^2 + \left(\frac{\bar{\omega}}{\eta}\frac{\delta_{scat}}{\sigma_{scat}^{aer}}\right)^2. \quad [5]$$

Based on this expression and the example values above, a coalbedo of $\eta = 0.1$ would have an error of 0.67 or 67%. Further reduction in the error via this approach (e.g., $\sigma_{ext}^{aer} - \sigma_{scat}^{aer}$) would be difficult. In contrast, if σ_{abs}^{aer} and σ_{scat}^{aer} are directly measured and their respective errors uncorrelated, a 5% error in each parameter would result in a fractional error in η of only 7%. In addition, since this methodology involves the attenuation of a calibrated light source, the shot noise for this measurement, which scales as the square root of the power reaching the detector, can be quite large. As a comparison, shot noise is significantly smaller for measurements of the scattering coefficient since this parameter can be acquired against a "black" background.

Clearly, an instrument that is capable of meeting the accuracy and precision requirements with minimal amount of post-processing and correction would be of value. One new class of instrument that addresses these issues is photoacoustic spectroscopy (e.g., Arnott et al. 2005; Lack et al. 2006; Droplet Measurement Technology, Boulder, CO) and, the subject of this article, photothermal interferometry (Sedlacek 2006). The hallmark of these approaches is that they *directly measure the aerosol absorption without interference from aerosol scattering* since their respective signals originate from the thermal dissipation of spectrally absorbed energy. Whereas photoacoustic spectroscopy (PAS) monitors the acoustic shockwave that is generated following absorption, photothermal interferometry (PTI) measures light absorption by following the refractive index change that accompanies the dissipation of the absorbed energy back to the surrounding air. Attractive features of the photothermal techniques for measuring aerosol absorption include its insensitivity to aerosol scattering, its ability to conduct the measurement without resort to deposition on a filter and the inherent high-sensitivity that enables near real-time response.

Photothermal interferometry (PTI) is particularly well suited for measuring very small changes in refractive index ($\Delta\phi \sim 10^{-11}$ rad, where $\Delta\phi$ is the refractive index phase shift) (e.g., Whinnery 1974; Campillo et al. 1981; Davis and Petuchowski 1982; Lin and Campillo 1985; Fluckiger et al. 1985; Moosmüller et al. 1997). However, despite being originally developed in the 1980's and even demonstrated by measuring aerosol absorption (Campillo and Lin 1983; Lin and Campillo 1985; Fluckiger et al. 1985), it has seen limited application (Dovichi 1990; Bialkowski 1996; Owens et al. 1999). This limited development/use can be primarily attributed to the sensitivity of some of these early optical designs to mechanical vibrations that required elaborate vibration isolation schemes. However, as discussed in detail elsewhere (Moosmüller et al. 1996; Sedlacek 2006), use of alternative interferometric configurations can reduce this noise contribution to manageable levels enabling this technique to be deployed in the field.

Below, we give brief background on the PTI technique and then present a detailed discussion of the experimental set up. This is followed by a presentation of calibration experiments using a molecular standard (NO_2), an intercomparison with a three-wavelength PSAP using laboratory-generated aerosols and finally, an extension of the intercomparison on ambient samples. We close with a prognosis on the performance of this technique with respect to the detection requirements needed.

THEORY

As a detailed discussion of the photothermal technique can be found elsewhere (Sedlacek 2006; Owens et al. 1999, Lin and Campillo 1985; Bialkowski 1996; Davis 1980; Davis and Petuchowski 1981; Dovichi 1990; Davis 1996), only the highlights that are relevant to the present discussion will be presented. At its most fundamental level, the PTI technique measures the *optical* pathlength change that one arm of an interferometer experiences (referred to as the "probe" arm) relative to the other arm of the interferometer (called the "reference"). When the two arms are recombined at a beamsplitter an interference pattern is created. If the optical pathlength in one arm of the interferometer changes, a commensurate shift in the interference pattern will take place. So sensitive are these interferometric techniques to pathlength changes they are routinely used in the field of metrology where sub-nanometer scales can be realized (Ishii et al. 1987; Downs 1990; Stone et al. 1999; Abou-Zeid and Wiese 1998). For the specific application of this technique for measuring light absorption, the optical pathlength change is induced when the dissipation of the spectrally absorbed energy creates a temperature gradient. This localized heating creates a refractive index gradient surrounding the particle (or molecule) causing the probe arm of the interferometer to take a slightly different optical pathlength relative to the unperturbed reference arm. This effect is analogous to solar heating of a road that creates a temperature gradient inducing the bending of light at oblique angles causing mirages (Bialkowski 1996). This altered optical pathlength results in a commensurate shift in the interference pattern at the beamsplitter that is then detected as a change in the signal intensity by a single element detector. By calibrating the interference pattern shift with an absorption standard, a change induced in the interferometer signal by aerosol absorption can be subsequently quantified. Since scattering does not create a temperature gradient, no refractive index gradient surrounding the aerosol is created; thus, the probe arm of the interferometer does not experience a pathlength change. The last is a critically important point because scattering is typically the dominant light extinction mechanism for nearly all aerosol types of interest to the climate change community.

For the interferometer of the type just described, it can be shown that the measured detector current (Davis 1980; Davis and Petuchowski 1981; Lin and Campillo 1985; Fluckiger et al.

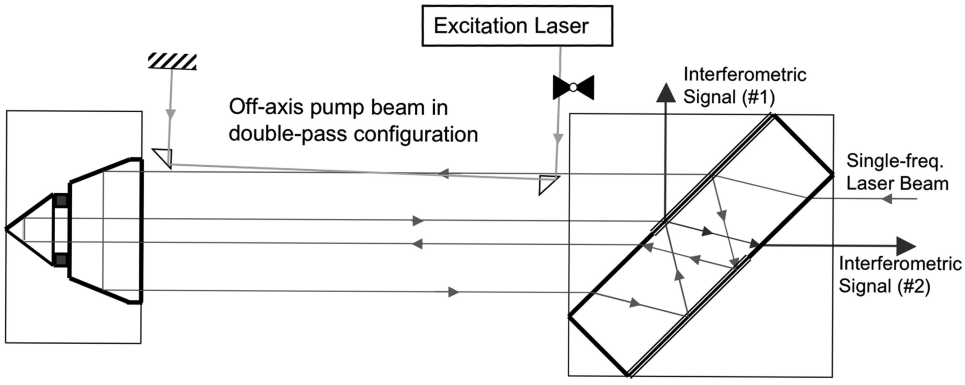

FIG. 1. Schematic of folded Jamin interferometer used for aerosol absorption measurements.

1985; Bialkowski 1996; Davis 1996; Owens et al. 1999; Sedlacek 2006), under quadrature conditions (i.e., $\phi_{\text{ref}} - \phi_{\text{probe}} = (2n+1)\,\pi/2$ where ϕ is the phase of each respective arm), reduces to

$$I(t) \propto \left(\frac{e\eta}{h\nu}\right) 2P_o \sin\Delta\phi(t) = \left(\frac{e\eta}{h\nu}\right) 2P_o \Delta\phi(t). \quad [6]$$

Here we have made the laser power in each arm of the interferometer the same ($P_o = P_{\text{probe}} = P_{\text{ref}}$) and have introduced factors that account for detector response, namely, e the electronic charge, η the detector quantum efficiency, $h\nu$ the laser energy and where $\Delta\phi(t)$ is the time-dependent induced phase fluctuations. This expression is valid in the limit of small $\Delta\phi(t)$, $\sin\Delta\phi(t) \approx \Delta\phi(t)$, (e.g., 1% level for $\Delta\phi \sim \pi/11$). As can be readily seen from Equation (6), in the limit of quadrature and small induced phase shifts, the PTI signal will be linearly dependent upon the induced phase shift created by the absorption of light by the particle.

Since the single-element detector monitors the amplitude of the interference pattern at the quadrature point, any event that results in a change in the relative pathlengths between the two arms of the interferometer will cause the pattern to shift. This shift can be generated through either the absorption of light or by mechanical vibrations of the optical components. While phase-sensitive detection techniques can be employed to narrow the detection bandwidth, such unwanted vibrations can still contribute noise that, in turn, can reduce the overall detection sensitivity. As a case in point, previous PTI configurations (Mach-Zehnder and modified Jamin) were limited to laboratory use precisely because of the sensitivity to mechanical vibrations, which effectively precluded use in field campaigns, and certainly aircraft deployment (Campillo and Lin 1983; Lin and Campillo 1985; Owens et al. 1999). Efforts to eliminate this sensitivity have included floating the optical table that supported the interferometer and encasing the interferometer inside an enclosure outfitted with acoustic attenuation material. In order to realize deployment of this technique outside the confines of a laboratory, an optical design that offered superior mechanical stability was sought. As discussed in detail elsewhere (Moosmüller and Arnott 1996; Moosmüller et al. 1996; Sedlacek 2006), a folded-Jamin interferometer design offers the desired robustness towards mechanical vibrations. Shown in Figure 1 is a schematic of the folded Jamin PTI unit used to measure aerosol light absorption. As is depicted in Figure 1, the incorporation of a retro-reflector, to fold the two-interferometer arms back to the etalon block, provides the "folded" Jamin design with superior optical resiliency to mechanical vibrations. The two halves of the width-wise split retro-reflector are connected together with PZT so that a controlling voltage could be sent to the PZT in order to maintain the requisite quadrature phase condition between the two arms of the interferometer.

Finally, it is to be noted that since aerosols have a small but nonvanishing heat capacity, there is a characteristic "heating time" following the absorption of light by the aerosols (Chan 1975). This heating time reflects the fact that the particle will heat up rapidly following light absorption but not transfer that heat to the surrounding air because of air's low conductivity (e.g., 0.026 $\text{W} \cdot \text{m}^{-1} \cdot \text{K}^{-1}$ at 298.2 K). After the particle has reached an equilibrium temperature, the energy initially taken in by the particle will then be imparted to the surrounding air. This characteristic time, T, first addressed by Chan (1975), is given by:

$$T = \frac{r^2 \rho_p C_p}{3K_a} \quad [7]$$

where r is the particle radius, ρ_p is the particle density, C_p is the specific heat of the particle, and K_a is the thermal conductivity of the surrounding air. Using carbon as an example, where $K_a = 0.026\ \text{W}\cdot\text{m}^{-1}\cdot\text{K}^{-1}$, $\rho_p = 2.25 \times 10^3\ \text{kg}\cdot\text{m}^{-3}$, $C_p = 714\ \text{J}\cdot\text{kg}^{-1}\cdot\text{K}^{-1}$ and $r = 1\ \mu\text{m}$, it is calculated that $T \sim 20\ \mu\text{sec}$ (Chan 1975), a time considerably faster than the conduction of the heated air. Hence, the efficient transfer of heat from micron-sized and smaller particles to the surrounding buffer gas makes PTI suitable for acquiring the optical properties of the aerosol in near real-time.

EXPERIMENTAL

The experiments undertaken in this study comprised three types: (1) fundamental performance measurements using a calibration standard, (2) performance intercomparison with a 3-wavelength PSAP involving laboratory-generated aerosols, where the particle diameter (D_p) and number density (N_p) could be easily controlled, and (3) the extension of the intercomparison to ambient aerosols. The laboratory-based intercomparison was undertaken so that complications associated with the complete removal of unwanted measurement artifacts (e.g., relative humidity effects on PSAP measurement; Schmid et al. 2006) could be controlled and thus eliminated. Following performance characterization against the PSAP, side-by-side measurement of ambient aerosols was undertaken.

PTI Calibration

Measurement of the photothermal signal is accomplished using phase-sensitive detection techniques where the output from a laser (in the present case an argon ion laser operating on the 514 nm line, Coherent FReD system, model: 300c) is modulated by a mechanical chopper (SR-450). The modulated photothermal signal is directed to a Stanford Research Systems lock-in amplifier/pre-amp combination (SR-850/SR-420) that is interfaced to a computer (Dell Latitude 820C) via GPIB. Typical time constants employed ranged from 10–30 seconds. Calibration of the PTI instrument was conducted by injecting a known concentration of NO_2 (Scott Gases, certified working class) into the sample cell and recording the signal as a function of injected concentration. NO_2 concentrations were generated by mixing the standard with dry nitrogen using mass flow controllers (Tylan). The accuracy of the mass flow meters is reported to be 1% full scale. Using propagation of errors methodology and measured signal fluctuations at the low end of the operation range for these mass flow meters (2%) it was determined that the uncertainty for the lowest concentrations is on the order of 10%. In order to minimize deposition of material on the turning prisms inside the PTI unit (Figure 1), a steady flow of dry N_2 (0.25 lpm) was directed towards the optic surface. However, the prisms surfaces were cleaned with methanol-wetted lens tissue periodically. The nominal pathlength, defined as the length over which the excitation beam overlaps a half-diameter of the probe arm of the interferometer, is found to be 5 cm.

PTI-PSAP Intercomparison Using Laboratory-Generated Aerosols

For the laboratory-based intercomparison the authors elected to aerosolize nigrosin which is a polyaniline-based black pigment that is commonly used for negative staining in bacteriology. Nigrosin was used instead of black carbon because: (1) it is an easily reproducible aerosol enabling inter-lab comparisons for systems that are not co-located (as compared to known issues with soot generation) and (2) aerosol morphology that has been shown to be spherical (Lack et al. 2006). In addition, nigrosin possesses a broad, featureless absorption spectrum in the visible making it an ideal BC surrogate. Bond et al. (1999) and more recently Lack et al. (2006) have also used aerosolized nigrosin for instrument characterizations (PSAP and PAS, respectively).

Aerosolization of an aqueous solution of nigrosin was accomplished using a commercial grade atomizer (constant output atomizer TSI, Model No. 3076). The nigrosin solution had a nominal concentration of 1 mg/cm^3. Following atomization, the particles were diffusion dried (TSI diffusion drier filled with desiccated silica gel, nominal bead size 2–5 mm with indicator: Grace). Since the atomizer generates a lognormal spread in particle size around a 90 nm mean, TSI's 3080L Electrostatic Classifier with 3081 Long Differential Mobility Analyzer (DMA) and impactor was used to size select the particles prior to injection into the spectrometer. Number concentration was measured with TSI model 3025A ultrafine condensation particle counter (CPC). After selecting a given particle diameter (D_p) and particle number density, the aerosol flow was then connected to the PTI until a stable signal was recorded after which the aerosol flow was redirected into the PSAP for a similar signal acquisition. Ancillary measurements were undertaken to correct for any particle loss inherent between the two inlets. The particle number density was measured both prior to and immediately following PSAP/PTI measurement. This procedure was repeated for several nigrosin D_ps and particle densities for a given D_p. Typical sample flow rates for the PSAP and PTI were 0.5–1.0 liter per minute (lpm).

The PSAP (Radiance, S/N:0020) was interfaced to a Dell Latitude computer via the COM1 port where the 1 Hz output was captured and logged. Prior to the intersystem comparison, PSAP flow rate was calibrated against a Dry Gas Meter (DryCal, DC-lite, SN:1784) and a digital flow meter (Omega, FMA-A2307 with readout standardized to 294.16K and 101.28 kPa). This calibration revealed that the actual flow differed from the reported flow by approximately 10%, thus the flow rate voltage reported by the PSAP was used to determine the flow in lpm that was subsequently used in offline data reduction. Furthermore, each time the filter was replaced, a careful measurement of the spot diameter was conducted. Typical spot size areas were 18.5 ± 0.48 mm^2 (95% confidence interval). A new filter was installed when the reported transmission dropped below 0.75, therefore the original Bond correction was employed (Virkkula et al. 2005). Since the Bond correction factors are valid for 550 nm it is important to ensure that reported absorption coefficients have been wavelength corrected to 550 nm before application of these correction factors (Bond et al. 1999). Therefore, the actual wavelengths of the 3-LEDs used in the PSAP needed to be measured. Using a medium resolution spectrometer (Ocean Optics USB2000 grating spectrometer, 3.5 nm spectral bandwidth) the central LED wavelengths were measured and found to differ from the manual's value by about 2% (actual/reported: 461.6/470; 522.7/530; 648.3/660). Accuracy of the spectrometer was confirmed by measuring the spectrum of a

Hg source whose spectral lines are well documented. These measured wavelengths were used when applying the Bond correction parameters. For the laboratory aerosols where the particle diameter could be controlled, the wavelength dependence correction assumed a $1/\sqrt{\lambda}$ dependence for particle diameters below 400 nm and a $1/\lambda$ dependence for larger D_ps. The following calibration transfer coefficients were used ($A = 0.866$ and $B = 1.317$).

PTI-PSAP Intercomparison of Ambient Aerosols

For measurement of ambient aerosol absorption a 5-cm diameter stainless steel inlet tube was erected outside our laboratory with its intake located 7.4 meters above the ground. Air was drawn in at nominally 50 liters per minute (l pm) using a scroll pump (Varian). Inside the laboratory a series of 2.5 cm tubes branching off the main inlet directed a fraction of the air to the PSAP, PTI and an integrating nephelometer (MRI model 1550 with an effective wavelength of 500 nm). Nominal flow rates for the optical instrumentation were 0.5–1 lpm. The nephelometer was calibrated with particle-free air ($\alpha_{scat} = 23$ Mm^{-1} @ $\lambda =$ 550 nm) and Freon-12 ($\alpha_{scat} = 360$ Mm^{-1} @ $\lambda = 550$ nm) and interfaced to a computer via an ADC card (IOTech, PCMCIA card, 16-bit) (Charlson et al. 1969). The ambient sample was heated prior to instruments sample inlets in an effort to reduce the effects of humidity. Prior to injection into the PTI instrument, the ambient stream was passed through a MnO_2 denuder (Thermo-Electron Corp.) to remove NO_2, which also absorbs 514 nm light.

RESULTS AND DISCUSSION

Laboratory-Based Measurements

As discussed above, the PTI method can be calibrated using commercially available and traceable gas standards. For the present effort, a certified concentration of NO_2 in air standard was used. As discussed elsewhere (Sedlacek 2006), knowledge of the NO_2 concentration and the absorption cross-section ($\sigma_{abs}^{NO_2} = 1.9\ (\pm 0.2) \times 10^{-19}$ cm^2/molecule) at 514 nm (Sedlacek 2006; Davidson et al. 1988 (Figure 2); Vandaele et al. 1998 (Figure 1); Vandaele et al. 1996 (Figure 1); Harder et al. 1997 (Figure 2)) allows a calibration curve of the PTI response as a function of absorption coefficient (α_{abs}, Mm^{-1}) to be readily generated. The NO_2 calibration curve used for these experiments is shown in Figure 2 where logarithmic plot is utilized to assist in resolving the lower concentrations. The slope is found to be 1.45 μV/Mm^{-1} with a standard deviation of 0.04 μV/Mm^{-1}. As expected from theory, the PTI signal is linear over the 4 decades of NO_2 concentrations used in these experiments ($R^2 = 0.9944$). Exploitation of NO_2 as a calibration standard is limited to wavelengths above 410 nm due to the opening up of the photodissociation channel that produces NO and O at shorter wavelengths (Okabe 1978). Uncertainty in the NO_2 absorption cross-section will propagate into the concentration measurement of BC through propagation of errors.

Another advantage of the calibration standard is that it allows the evaluation of the performance of this instrument without the complications associated with aerosol generation (e.g., maintaining a steady concentration with a steady size distribution).

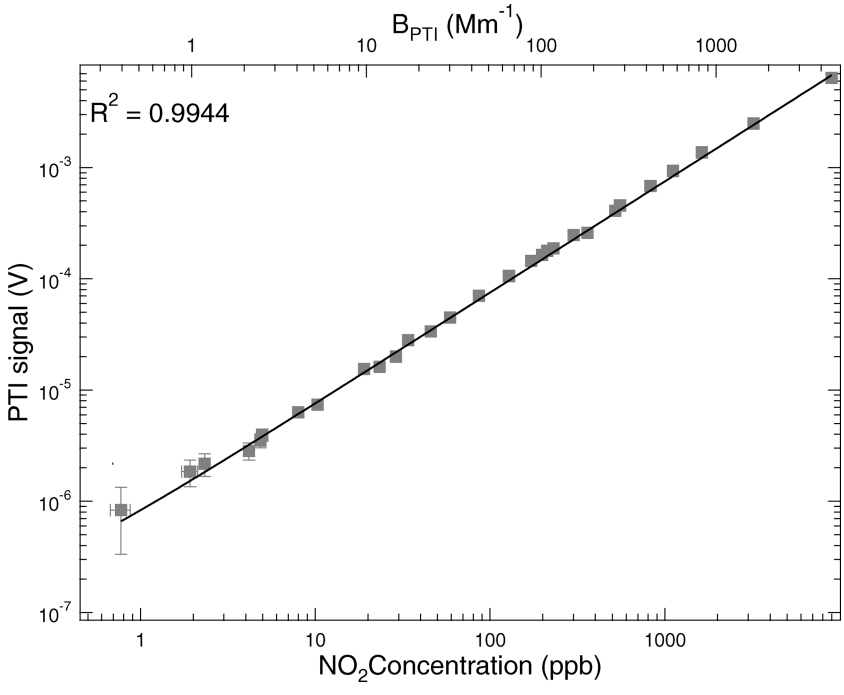

FIG. 2. PTI Calibration plot using NO_2.

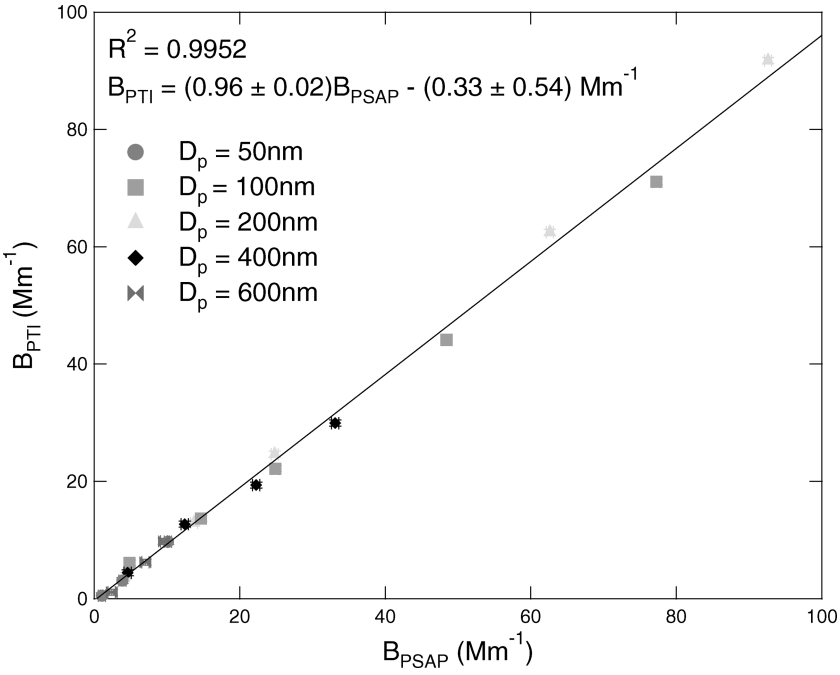

FIG. 3. Plot of nigrosin absorption coefficients measured by PTI and PSAP.

The least squares fit provides the calibration slope along with a measure of the standard deviation. From this slope, it is estimated that the 95% confidence interval for accuracy is on the order of 5%. As discussed earlier, the characteristic time for heat dissipation of the absorbed laser light by the aerosol particles is sufficiently short (microseconds) that the PTI calibration curve generated using a molecular standard will be valid. The PTI precision, defined here as $\pm 2\sigma$, was estimated by measuring the standard deviation from a 198 ppb loading of NO_2 and found to be 0.16 Mm^{-1} for a 10-second time constant. Assuming that the PTI signal is dominated by shot noise, the one-second precision of 1.4 Mm^{-1} for ammonia reported by Owens et al. (1999) translates to 0.44 Mm^{-1} for a 10-second time constant indicating the improved performance of the folded Jamin design. The reader is reminded that Owens et al. (1999) used a modified Jamin configuration where two etalon blocks were used. Also it should be noted that at 9.22 microns ammonia has a cross-section that is nominally an order of magnitude larger than the cross-section for NO_2 at 514 nm ($\sigma_{\text{abs}}^{\text{ammonia}} = 2.1 \times 10^{-18}$ cm^2/molecule @ 9.22 microns, Brewer et al. 1978). Finally a lower detection limit for the folded Jamin PTI is estimated to be 0.35 Mm^{-1} for a 10 second time constant.

While the goal is to measure the absorption coefficient of ambient aerosols, the first order of business is to calibrate the performance of the PTI technique against the PSAP, which, because of its ubiquity in the field has become the *de facto* standard.[1] The inter-instrument comparison described below was conducted by measuring the absorption coefficient for laboratory-generated nigrosin aerosols as a function of particle diameter, D_p.

For the intercomparison a known concentration of size-selected nigrosin aerosols were injected into the PTI and the PSAP. Several diameter of nigrosin particles (D_p) were selected and a plot of nigrosin absorption coefficient measured by the PTI, B_{PTI}, versus that measured by the PSAP, B_{PSAP}, is shown in Figure 3. The particle number densities chosen for this intercomparison were based on generating absorption coefficients at atmospherically relevant levels (0–50 Mm^{-1}). While a very slight bias towards the PSAP is observed in the slope (0.96 ± 0.02), the agreement observed between the two instruments is excellent as evidenced by both the slope very near unity and high correlation coefficient ($R^2 = 0.9952$). It is important to stress that this comparison was conducted on dried nigrosin aerosols, so differences that might be expected due to humidity effects, either cellulose substrate swelling or additional scattering corrections, were eliminated (Arnott et al. 2003; Schmid et al. 2006).

Since nigrosin aerosols can be reproducibly generated they enable the comparison between instrumentation that *are not* co-located. In the present case, a comparison with a photoacoustic spectrometer system (another photothermal-based technique) can be undertaken to further validate the PTI performance. Measurement of the PTI signal as a function of nigrosin number density for a given particle diameter (D_p) gives a slope that is equal to the absorption cross-section (σ_{abs}, cm^2/particle). Plotted in Figure 4 is the measured absorption cross-section for nigrosin aerosols from several manufacturers as a function of particle diameter along with the published data by Lack and co-workers

[1]It is to be noted that the PSAP is being more closely scrutinized as evidenced by the work of Subramanian et al. (2007) and Springston and Sedlacek (2007).

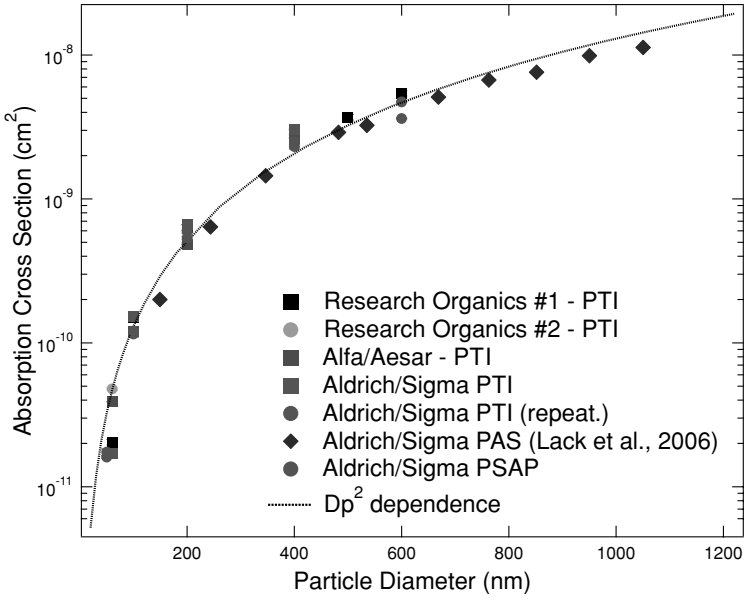

FIG. 4. Measured nigrosin absorption cross-section as a function of particle diameter.

(2006). The reason for looking at nigrosin from several manufacturers was due to the fact that the commercially available "nigrosin" is actually a mixture of the polyaniline nigrosin pigment (which is bluish/black color) with an orange dye. The ratio between these two chemicals is subsequently adjusted to achieve a specific color index (CI: 50420) and so it was thought that this could lead to differing absorption cross-sections. However, while aqueous solutions of nigrosin from different manufacturers do indeed give slightly different visible absorption spectra this difference was negligible in the 500–550 nm region. For completeness, the absorption cross-section measured using the PSAP is also plotted in Figure 4. As can be readily seen, the agreement between the three techniques is quite good. It is interesting to note that the absorption cross-section primarily goes as the square of the particle radius (as opposed to cube) indicating that the particles do not act as volume absorbers (Rayleigh regime) but as surface absorbers (geometric optics regime). Artifacts associated with relative humidity (RH) have been minimized in this part of the study in order to simplify the comparison (Arnott et al. 2003; Raspet et al. 2003; Schmid et al. 2006). Finally, we wish to stress the utility of using nigrosin as a soot surrogate. As evidenced herein, nigrosin enables informal intercomparisons among instruments that are not co-located to be readily undertaken because aerosolization of nigrosin can be easily reproduced and does not suffer from morphological complexities common with soot generation such as fractal collapse.

Ambient Aerosol Measurements

The PSAP and the PTI units were attached to an ambient sampling tube. The intercomparison started in December 2006 and lasted through February 2007. Depicted in Figure 5 is a 12-minute running average of aerosol absorption measured by the PTI and PSAP for the month of February. Breaks in the data acquisition were due to either ongoing PTI unit improvements or for execution of the aforementioned laboratory-based experiments. As can be clearly discerned, the PTI correlates with the PSAP very well for most of the intercomparison episode. Notable discrepancies between the two units show up during high humidity conditions, as will be discussed in more detail below. In Figure 6, we have isolated a specific 12-hour period to look more closely at the correlation between the two instruments under high temporal resolution conditions (10-sec time constants). In this figure, we have also overlaid the measured aerosol scattering coefficient by an integrating nephelometer. Here we have again just shown the "green" channel (522.7 nm) from the PSAP, which has been wavelength corrected to 514 nm. As can be seen, all three instruments show pronounced correlation. The single scattering albedo (SSA), plotted in the top frame of the figure, was calculated using the PTI data. The lower frame in Figure 6 quantifies the correlation between the PTI and PSAP where a plot of the PTI signal versus the PSAP results in slope of 1.03 ± 0.01. This slope agrees well with that measured in the laboratory using nigrosin where a slight bias is observed towards the PTI.

The mean absorption coefficient for the entire December-February sampling period was found to be 3.7 with a variability of 3.1 Mm^{-1}. Over the same sampling period the mean scattering coefficient reported by the nephelometer was found to be 54 with a variability of 30 Mm^{-1}. Finally, the mean scattering and absorption coefficients reported here can be used to provide a measure of the single scattering albedo for this sampling period (December–February) and is estimated to be 0.94 with a variability of 0.06.

While the agreement between the PSAP and the PTI for both the laboratory and ambient aerosols measurements is quite

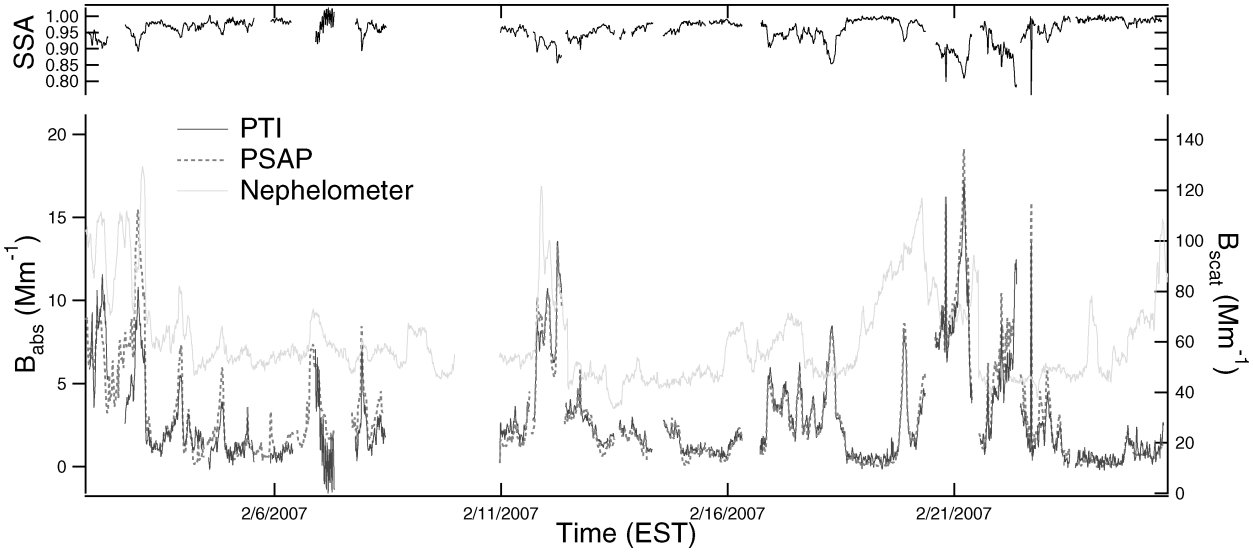

FIG. 5. Month long measurement campaign of ambient Aerosol Absorption and scattering.

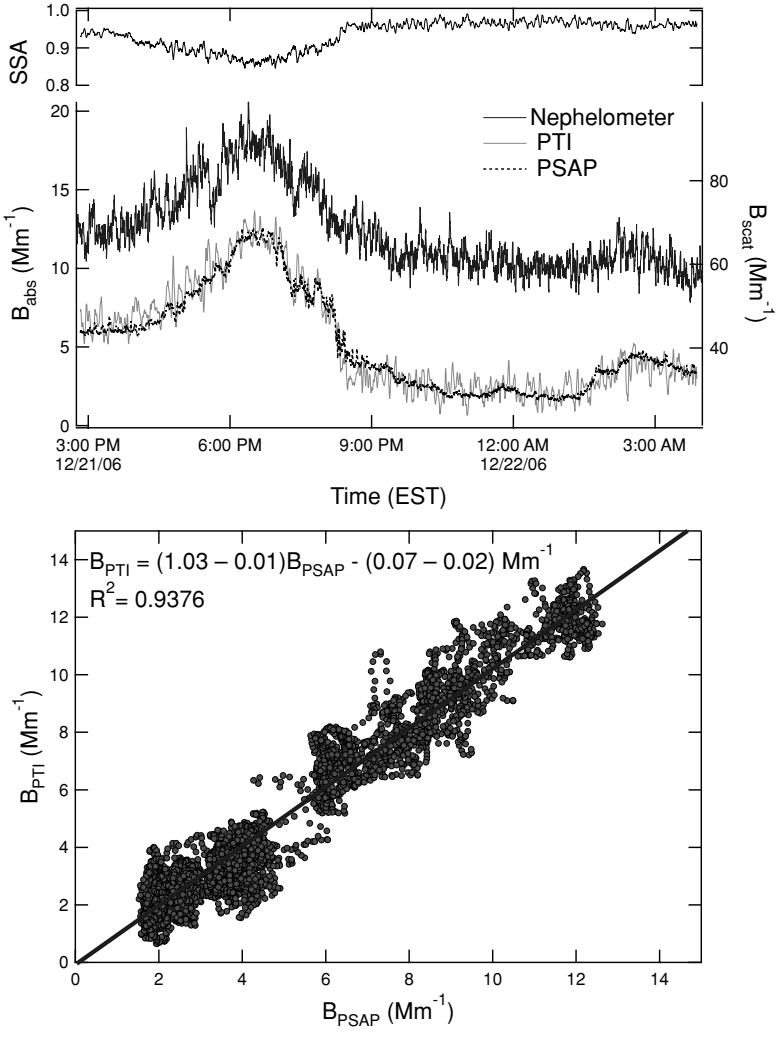

FIG. 6. High-temporal resolution measurement of aerosol absorption.

encouraging, it needs to be stressed that this comparison was for dried laboratory-generated aerosols and ambient aerosols which, on average, were sampled under relative humidity <50%. However during the ambient intercomparison phase of this work, there were periods of very high humidity (100%) where marked differences were observed between the PSAP and the PTI. An example of this deviation is shown in the Figure 7 where the absorption coefficient measured by the PSAP and PTI along with the measured relative humidity is shown for a two-day period of constant rain along with the correlation plot between the PTI and PSAP. The data shown in Figure 7 is a 12 minute running average. As can be readily seen, under high humidity conditions the absorption coefficient reported by the PSAP is higher than that reported by the PTI. Arnott and co-workers (2003) have observed similar behavior during an intercomparison between the PSAP and their photoacoustic spectrometer. The observed behavior can be qualitatively understood by examining how each technique reacts to a wet sample. In the case of the PSAP, the hydrophilic nature of the cellulose membrane upon which the glass fiber is supported (Pallflex type E70.2075W) can potentially cause the membrane to swell upon exposure to water and thereby decrease the amount of transmitted light (Arnott et al.

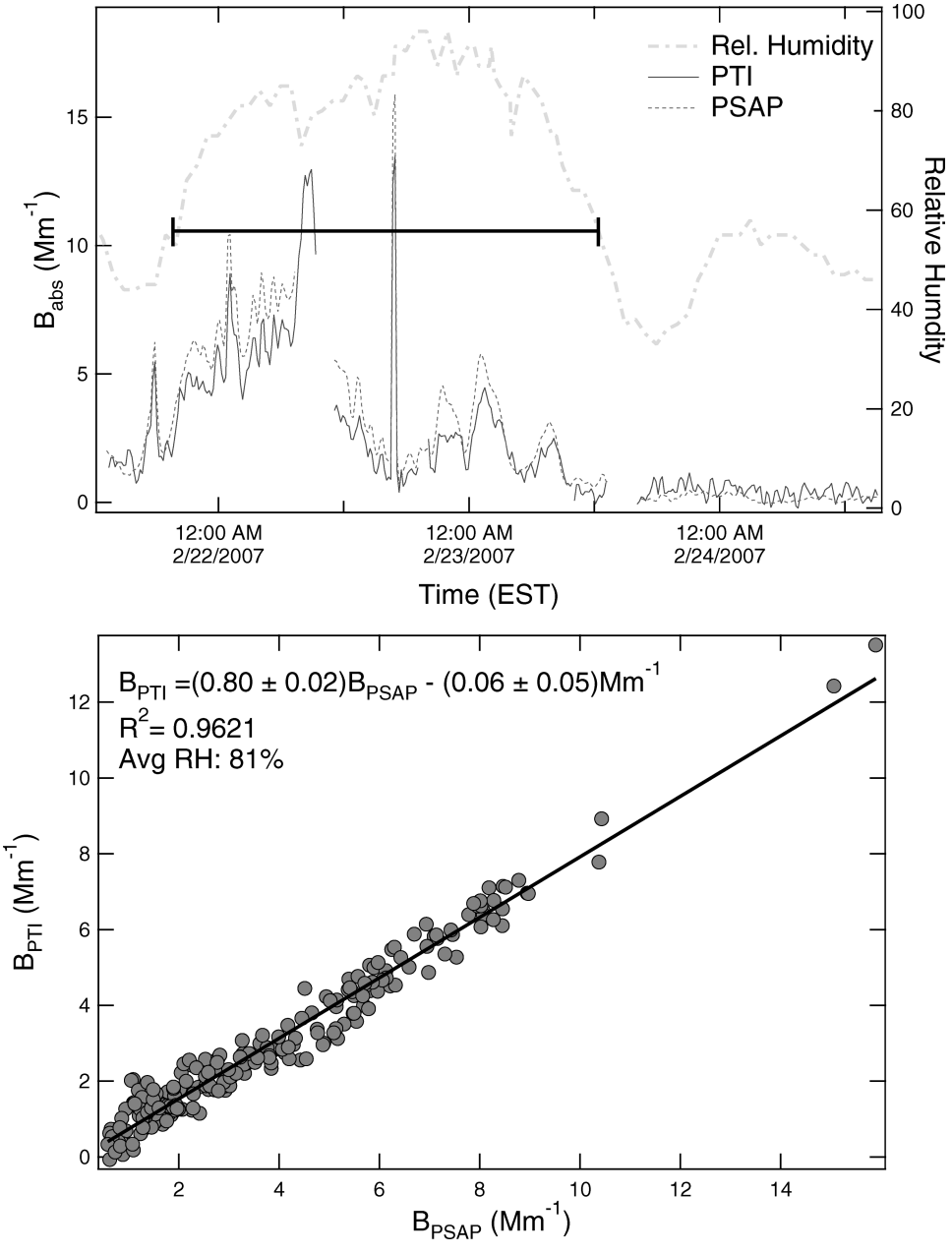

FIG. 7. Measurement of ambient aerosol absorption during high humidity conditions.

2003). Schmid et al. (2006) applied a RH-dependent correction factor (a second order polynomial) to their PSAP in an effort to confront this issue. Photothermal approaches such as PTI, PAS, or photothermal deflection can also have RH related issues attributable to latent heat. Specifically, and as discussed quite nicely by Arnott et al (2003) and Raspet et al. (2003), light absorption by a water-coated BC core can result in the mass transfer for water molecules from the water layer surrounding the core to the vapor surrounding the particle. In the case of the PTI approach, which measures the change in the index of refraction, this influx of water molecules causes the refractive index to increase thereby offsetting the decrease in the refractive index caused by heating. While this issue is presently being addressed in our laboratory and will be the subject of an upcoming paper, experiments carried out by Arnott and co-workers suggests that the effects of this mass transfer becomes a concern for RHs $>70\%$.

These intercomparisons provide confidence in the performance of the PTI techniques towards aerosol absorption measurements. Since this instrument represents a first generation, there are a few straightforward tasks that can be taken to improve the performance of the instrument. Two such tasks that are presently underway include the incorporation of a parabolic return mirror to reflect the excitation beam back into the sample cell thus giving a double pass of the excitation beam thereby increasing of the pathlength from nominal 5 cm to 10 cm (while still keeping the instrument footprint within that of a standard instrument rack). Another high priority improvement will be to incorporate a multispectral capability. One approach is to co-propagate into the sample cell several pump wavelengths of interest where each wavelength is modulated at a unique frequency that is not an integer of another modulation frequency. The resultant data set could then be demodulated using either multiple lock-in amplifiers or by taking the Fourier transformation from temporal space to frequency space. This approach can be extended to any number of pump wavelengths.

All instruments either presently deployed or under development have the requisite sensitivity towards aerosol absorption in atmospherically relevant range <25 Mm^{-1} (Sheridan et al. 2005). While the measurement precision for all the techniques are sensitive to the time constant, as is discussed elsewhere, a differential technique such as the PSAP displays a significant departure from $1/\sqrt{t}$ (Springston and Sedlacek 2007). This can become an issue when the temporal constraints for the measurement scenario require very fast time measurements, as would be needed to conduct microstructure study of urban or biomass plumes using aircraft. Both the PTI and PAS uncertainties (Lack et al. 2006; Arnott et al. 1999) follow $1/\sqrt{t}$.

CONCLUSION

We have discussed the application of the photothermal interferometry technique towards the challenge of directly measuring aerosol absorption *in situ*. A description of the folded Jamin interferometer design along with supporting data has been presented. Excellent agreement is observed in a comparison of reported absorption coefficients measured by the PTI unit and a particle soot absorption photometer (PSAP) utilizing laboratory-generated nigrosin aerosols. Extension of this intercomparison to ambient aerosols also gives very good correlation between the two instruments. However, under high RH conditions significant deviation is observed and is ascribed to the hydrophilic nature of the cellulose filter substrate that swells upon exposure to high RH conditions and mass transfer issues associated with the PTI technique. The PTI approach presently under development in our laboratory will enable the requisite detection sensitivity to be realized with a time response that is compatible with aircraft deployment.

REFERENCES

Abou-Zeid, A., and Wiese, P. (1998). Interferometer with a Wavelength-Tuned Diode Laser for Surface Profilometry, *Meas. Sci. Technol.* 9:1105–1110.

Anderson, A. L., Masonis, S. J., Covert, D. S., Ahlquist, N. C., Howell, S. G., Clarke, A. D., and McNaughton, S. (2003). Variability of Aerosol Optical Parameters Derived from in Situ Aircraft Measurements During ACE-Asia, *J. Geophys. Res.* 108:D23 8647–8666.

Arnott, W. P., Hamasha, K., Moosmüller, H., Sheridan, P. J., and Ogren, J. A. (2005). Towards Aerosol Light Absorption Measurements with a 7-Wavelength Aethalometer: Evaluation with a Photoacoustic Instrument and a 3 Wavelength Nephelometers, *Aerosol Sci. Technol.* 39:17–39.

Arnott, W. P., Moosmüller, H., Sheridan, P. J., Ogren, J. A., Raspet, R., Slaton, W. V., Hand, J. L., Kreidenweis, S. M., and Collett Jr., J. L. (2003). Photoacoustic and Filter-Based Ambient Aerosol Light Absorption Measurements: Instrument Comparisons and the Role of Humidity, *J. Geophys. Res.* 108:D1 4034.

Arnott, W. P., Moosmüller, H., and Walker, J. W. (2000). Nitrogen Dioxide and Kerosene-Flame Soot Calibration of Photoacoustic Instruments for Measurement of Light Absorption by Aerosols, *Rev. Sci. Instru.* 71:4545–4552.

Arnott, W. P., Moosmüller, H., Rogers, C. F., Jin, T., and Bruch, R. (1999). Photoacoustic Spectrometer for Measuring Light Absorption by Aerosol: Instrument Description, *Atmos. Environ.* 33: 2845–2852.

Bevington, P. R. (1969). *Data Reduction and Error Analysis for the Physical Sciences*, McGraw-Hill, New York.

Bialkowski, S. E. (1996). Photothermal Spectroscopy Methods for Chemical Analysis, Vol. 134, *Chemical Analysis: A Series of Monographs on Analytical Chemistry and its Application,* John Wiley and Sons Publisher, New York, and references therein.

Bond, T. C., Anderson, T. L., and Campbell, D. (1999). Calibration and Intercomparison of Filter–Based Measurements of Visible Light Absorption by Aerosols, *Aero. Sci. Technol.* 30:582–600.

Bond, T. C., and Bergstrom, R. W. (2006). Light Absorption by Carbonaceous Particles: An Investigative Review, *Aerosol Sci. Technol.* 40:27–67.

Bond, T. C., Habib, G., and Bergstrom, R. W. (2006). Limitations in the Enhancement of Visible Light Absorption Due to Mixing State, *J. Geo. Phys.* 111: D20211.

Campbell, D., Copeland, S., and Cahill, T. (1995). Measurement of Aerosol Absorption Coefficient from Teflon Filters using Integrating Plate and Integrating Sphere Techniques, *Aerosol Sci. Technol.* 22:287–292.

Campillo, A. J., Dodge, C. F., and Lin, H.-B. (1981). Aerosol Particle Absorption Spectroscopy by Photothermal Modulation of Mie Scattered Light, *Appl. Opt.* 20:3100–3102.

Campillo, A. J., and Lin, H.-B. (1983). Method and Apparatus for Aerosol Particle Absorption Spectroscopy, *U.S. Patent* 4,415,265.

Chan, C. H. (1975). Effective Absorption for Thermal Blooming Due to Aerosols, *Appl. Phys. Lett.* 26:628–630.

Charlson, R. J., Ahlquist, N. C., Selvdge, H., and MacCready, P. B. (1969). Monitoring of Atmospheric Aerosol Parameters with the Integrating Nephelometer, *J. Air Pollution Control Assoc*. 19:937–942.

Charlson, R. J., Langner, J., Rodhe, H., Leovy, C. B., and Warren, S. G. (1991). Perturbation of the Northern Hemisphere Radiative Balance by Backscattering From Anthropogenic Sulfate Aerosols, *Tellus* 43A:152–163.

Charlson, R. J., Schwartz, S. E., Hales, J. M., Cess, R. D., Coakley, J. A., Hansen, J. E., and Hofmann, D. J. (1992). Climate Forcing by Anthropogenic Aerosols, *Science* 255:423–430.

Chylek, P., and Wong, J. (1995). Effect of Absorbing Aerosols on Global Radiation Budget, *Geophys. Res. Lett*. 22:929–931.

Davidson, J. A., Cantrell, C. A., McDaniel, A. H., Shetter, R. E., Madronich, S., and Calvert, J. G. (1988). Visible-Ultraviolet Absorption Cross Sections for NO_2 as a Function of Temperature, *J. Geophys. Res*. 93:7105–7112.

Davis, C. C. (1996). *Laser and Electro-Optics—Fundamentals and Engineering*, Cambridge University Press, New York.

Davis, C. C. (1980). Trace Detection in Gases Using Phase Fluctuation Optical Heterodyne Spectroscopy, *Appl. Phys. Lett*. 36:515–518.

Davis, C. C., and Petuchowski, S. J. (1981). Phase Fluctuation Optical Heterodyne Spectroscopy of Gases, *Appl. Opt*. 20:2539–2554 and errata: *Appl. Opt*. 20:4151.

Dovichi, N. J. (1990). Laser-based Microchemical Analysis, *Rev. Sci. Instrum*. 61:3653–3667.

Downs, M. J. (1990). A Proposed Design for an Optical Interferometer with Sub-Nanometric Resolution, *Nanotechnology* 1:27–30.

Fluckiger, D. U., Lin. H.-B., and Marlow, W. H. (1985). Composition Measurement of Aerosols of Submicrometer Particles by Phase Fluctuation Absorption Spectroscopy, *Appl. Optics* 24:1668–1681.

Hallar, A. G., and Strawa, A. W. (2004). In Situ Measurements of Aerosol Optical Properties with an Emphasis on Spectral Properties of Carbonaceous Aerosols, *Proceedings SOFIA Upper Deck Science Opportunities Workshop*, NASA Ames Research Center, Moffett Field, CA.

Hansen, J. E., Sato, J., and Ruedy, R. (1997). Radiative Forcing and Climate Response, *J. Geophys. Res*. 102:6831–6864.

Hansen, J. E., Sato, J., Lacis, A., Ruedy, R., Tegen, I., and Matthews, E. (1998). Climate Forcing in the Industrial Era, *Proc. Natl. Acad. Sci*. 95:12753.

Harder, J. W., Brault, J. W., Johnston, P. V., and Mount, G. H. (1997). Temperature Dependent NO_2 Cross-Sections a High Spectral Resolution, *J. Geophys. Res*. 102:3861–3879.

Haywood, J. M., and Shine, K. P. (1995). The Effect of Anthropogenic Sulfate and Soot Aerosol on the Clear Sky Planetary Radiation Budget, *Geophys. Res. Lett*. 22:603–606.

Haywood, J. M., Ramaswamy, V., and Soden, B. J. (1999). Tropospheric Aerosol Climate Forcing in Clear-Sky Satellite Observations over the Oceans, *Science* 283:1299–1303.

Ishii, Y., Chen, J., and Murata, K. (1987). Digital Phase–Measuring Interferometry with a Tunable Laser Diode, *Opt. Lett*. 12:233–235.

Kaufman, Y. J., Tanré, D., Holben, B. N., Mattoo, S., Remer, L. A., Eck, T. F., Vaughan, J., and Chetenet, B. (2002). Aerosol Radiative Impact on Spectral Solar Flux at the Surface, Derived From Principal-Plane Sky Measurements, *J. Atmos. Sci*. 59:635–646.

Lack, D. A., Lovejoy, E. R., Baynard, T., Pettersson, A., and Ravishankara, A. R. (2006). Aerosol Absorption Measurement using Photoacoustic Spectroscopy: Sensitivity, Calibration, and Uncertainty Developments, *Aerosol Sci. Technol*. 40:697–708.

Lee, W.-K., Güngör, A., Ho, P.-T., and Davis, C. C. (1985). Direct Measurement of Dilute Dye Solution Quantum Yield by Photothermal Laser Heterodyne Interferometry, *Appl. Phys. Lett*. 47:916–918.

Lin, C.-I., Baker, M., and Charlson, R. J. (1973). Absorption Coefficient of Atmospheric Aerosol: A Method for Measurement, *Appl. Opt*. 12:1356–1363.

Lin, H.-B., and Campillo, A. J. (1985). Photothermal Aerosol Absorption Spectroscopy, *Appl. Optics,* 24:422–433.

Lohmann, U., and Feichter, J. (2001). Can the Direct and Semi-Direct Aerosol Effect Compete with the Indirect Effect on a Global Scale, *Geophys. Res. Lett*. 28:159–161.

Mazzoni D. L., and Davis C. C. (1991). Trace Detection of Hydrazines by Optical Homodyne Interferometry, *Appl. Optics*, 30:756–764.

Mikhailov, E. F., Vlasenko, S. S., Podgorny, I. A., Ramanathan, V., and Corrigan, C. E. (2006). Optical Properties of Soot-Water Drop Agglomerates: An Experimental Study, *J. Geophys. Res*. 111:D07209.

Moosmüller, H., and Arnott, W. P. (1996). Folded Jamin Interferometer: A Stable Instrument for Refractive-Index Measurements, *Opt. Lett*. 21:438–440.

Moosmüller, H., Arnott, W. P., and Roger, C. F. (1997). Methods for Real-Time, In Situ Measurement of Aerosol Light Absorption, *J. Air and Waste Management Assoc*. 47:157–166.

Moosmüller, H., Varma, R., and Arnott, W. P. (2005). Cavity Ring-down and Cavity-Enhanced Detection Techniques for the Measurement of Aerosol Extinction, *Aerosol Sci. Technol*. 39:30–39.

Okabe, H. (1978). *Photochemistry of Small Molecules*, John Wiley and Sons, New York.

Owens, M. A., Davis, C. C., and Dickerson, R. R. (1999). A Photothermal Interferometer for Gas–Phase Ammonia Detection, *Anal. Chem*. 71:1391–1399.

Petzold, A., and Schönlinner, M. (2004). Multi-angle Absorption Photometry—A New Method for the Measurement of Aerosol Light Absorption and Atmospheric Black Carbon, *J. Aerosol Sci*. 35:421–441.

Petzold, A., Kramer, H., and Schönlinner, M. (2002). Continuous Measurement of Atmospheric Black Carbon Using a Multi-Angle Absorption Photometer, *Environ. Sci. Pollut. Res*. 4:78–82.

Raspet, R., Slaton, W. V., Arnott, W. P., and Moosmüller, H. (2003). Evaporation—Condensation Effects on Resonant Photoacoustics of Volatile Aerosols, *J. Atmos. Ocean. Technol*. 20:685–695.

Sappey, A. D., Hill, E. S., Settersten, T., and Linne, M. A. (1998). Fixed-Frequency, Cavity Ringdown for Atmospheric Particulate Matter, *Optic Lett*., 23:954–956.

Schmid, O., Artaxo, P., Arnott, W. P., Chand, D., Gatti, L. V., Frank, G. P., Hoffer, A., Schnaiter, M., and Andreae, M. O. (2006). Spectral Light Absorption by Ambient Aerosols Influenced by Biomass Burning in the Amazon Basin. I: Comparison and Field Calibration of Absorption Measurement Techniques, *Atmos. Chem. Phys*. 6:3443–3462.

Schwartz, S. E. (2004). Uncertainty Requirements in Radiative Forcing of Climate Change, *Air & Waste Mange. Assoc*. 54:1351–1359.

Sedlacek, A. J. (2006). Real-Time Detection of Ambient Aerosols using Photothermal Interferometry: Folded Jamin Interferometer, *Rev. Sci. Instrum*. 77:064903.

Sheridan, P. J., Arnott, W. P., Ogren, J. A., Andrews, E., Atkinson, B. D., Covert, D. S., Moosmüller, H., Petzold, A. Schmid, B., Strawa, A. W., Varma, R., and Virkkula, A. (2005). The Reno Aerosol Optics Study: An Evaluation of Aerosol Absorption Measurement Methods, *Aerosol Sci. Technol*. 39:1–16.

Smith, J. D., and Atkinson, D. B. (2001). A Portable Pulsed Cavity Ring-Down Transmisson Meter for Measurement of the Optical Extinction of the Atmospheric Aerosol, *Analyst*, 126:1210–1216.

Springston, S. R., and Sedlacek, A. J. (2007). Towards a Better Understanding of PSAP Noise, *Aerosol Sci. Technol*. (submitted for publication)

Stone, J. A., Stejskal, A., and Howard, L. (1999) Diode Lasers in Length Metrology: Application to Absolute Distance Interferometry, *International J. Metrology* Nov–Dec:1–7.

Strawa, A. W., Castaneda, R., Owano, T., Baer, D. S., and Paldus, B. A. (2003). The Measurement of Aerosol Optical Properties Using Continuous Wave Cavity Ring-down Techniques, *J. Atmos. Ocean. Technol*. 20:454–465.

Subramanian, R., Roden, C. A., Boparai, P., and Bond, T. C. (2007). Yellow Beads and Missing Particles: Trouble Ahead for Filter-Based Absorption Measurements, *Aerosol Sci. Tech*. 41:630–637.

Vandaele, A. C., Hermans, C., Simon, P. C., Van Roozendael, M., Guilmot, J. M., Carleer, M., and Colin, R. (1996). Fourier Transform Measurement of NO_2 Absorption Cross-Section in the Visible Range at Room Temperature, *J. Atmos. Chem.* 25:289–305.

Vandaele, A. C., Hermans, C., Simon, Carleer, M., Colin, R., Fally, S., Mérienne, Jenouvrier, A., and Coquart, B. (1998). Measurements of the NO_2 Absorption Cross-section from 42000 cm^{-1} to 10000 cm^{-1} (238–1000 nm) at 220 K and 294 K, *J. Quant. Spectrosc. Radiat. Transf.* 59:171–184.

Vander Wal, R. L., and Ticich, T. M. (1999). Cavity Ringdown and Laser-Induced in Candescence Measurements of Soot, *Appl. Optics*, 38:1444–1451.

Vinoj, V., Babu, S. S., Satheesh, S. K., Moorthy, K. K., and Kaufman, Y. J. (2004). Radiative Forcing by Aerosols Over the Bay of Bengal Region Derived from Shipborne, Island-based, and Satellite (Moderate-Resolution Imaging Spectroradiometer) Observations,*J. Geophys. Res.* 109:D05203.

Virkkula, A., Ahlquist, N. C., Covert, D. S., Arnott, W. P., Sheridan, P. J., Quinn, P. K., and Coffman, D. J. (2005). Modification, Calibration and a Field Test of an Instrument for Measuring Light Absorption by Particles, *Aerosol Sci. Technol.* 39:68–83.

Whinnery, J. R. (1974). Laser Measurement of Optical Absorption of Liquids, *Accounts Chem. Res.*, 7:225–231.